Cancer Biology and Signal Transduction

Molecular Cancer Therapeutics

Involvement of microRNA-24 and DNA Methylation in Resistance of Nasopharyngeal Carcinoma to Ionizing Radiation

Sumei Wang[1,2], Rong Zhang[1,3], Francois X. Claret[2,4], and Huiling Yang[1]

Abstract

Nasopharyngeal carcinoma (NPC) is a malignant tumor originating in the epithelium. Radiotherapy is the standard therapy, but tumor resistance to this treatment reduces the 5-year patient survival rate dramatically. Studies are urgently needed to elucidate the mechanism of NPC radioresistance. Epigenetics—particularly microRNAs (miRNA) and DNA methylation—plays an important role in carcinogenesis and oncotherapy. We used qRT-PCR analysis and identified an miRNA signature from differentially expressed miRNAs. Our objectives were to identify the role of miR24 in NPC tumorigenesis and radioresistance and to identify the mechanisms by which miR24 is regulated. We found that miR24 inhibited NPC cell growth, promoted cell apoptosis, and suppressed the growth of NPC xenografts. We showed that miR24 was significantly downregulated in recurrent NPC tissues. When combined with irradiation, miR24 acted as a radiosensitizer in NPC cells. One of the miR24 precursors was embedded in a CpG island. Aberrant DNA methylation was involved in NPC response to radiotherapy, which linked inactivation of miR24 through hypermethylation of its precursor promoter with NPC radioresistance. Treating NPC cells with the DNA-hypomethylating agent 5-aza-2′-deoxycytidine compensated for the reduced miR24 expression. Together, our findings showed that miR24 was negatively regulated by hypermethylation of its precursor promoter in NPC radioresistance. Our findings defined a central role for miR24 as a tumor-suppressive miRNA in NPC and suggested its use in novel strategies for treatment of this cancer. *Mol Cancer Ther; 13(12); 3163–74. ©2014 AACR.*

Introduction

Nasopharyngeal carcinoma (NPC) is a nonlymphomatous squamous cell carcinoma (SCC) that occurs in the epithelial lining of the nasopharynx. This Epstein–Barr virus (EBV)-associated epithelial malignancy is prone to local invasion and early distant metastasis. NPC is prevalent in Southern China, especially in the Cantonese region around Guangzhou, where the incidence is approximately 30–80/100,000 persons per year (1–3). Studies have shown that a variety of genetic, ethnic, and environmental factors contribute to the development of NPC (1, 4–6). Radiotherapy is the standard treatment for NPC. However, the tumor often develops resistance to ionizing radiation (IR) and the relapse rate is as high as 82%, so radioresistance is a major cause of treatment failure (7, 8), leading to incomplete cure, recurrence, or metastasis. Once NPC reoccurs or metastasizes, patients have a very limited 5-year survival rate. Therefore, understanding the mechanism of NPC radioresistance is urgently needed to improve the effectiveness of NPC therapy and patient survival rates.

The role of epigenetic modification, especially the microRNAs (miRNA or miRs) and DNA methylation, has been extensively explored in the pathogenesis of cancer (9–11). First discovered as a mechanism of gene regulation in *Caenorhabditis elegans*, miRNAs are a class of endogenous noncoding RNA molecules about 22 nucleotides in length (12, 13) and may regulate more than 60% of genes in multicellular eukaryotes (14, 15). miRNAs control gene expression by binding to the 3′ untranslated region (UTR), 5′UTR, or coding region of mRNAs, leading to mRNA degradation or translational repression (16). Many miRNAs exist in clusters, such as miR23∼27∼24. Three fourths of the miRNA genes in the database miRBase R19 are assigned to miRNA families (17).

[1]Department of Pathophysiology, Zhongshan School of Medicine, Sun Yat-Sen University, Guangzhou, Guangdong, P.R. China. [2]Department of Systems Biology, The University of Texas MD Anderson Cancer Center, Houston, Texas. [3]State Key Laboratory of Oncology in South China, Sun Yat-Sen University, Guangzhou, Guangdong, P.R. China. [4]Experimental Therapeutics Academic Program and Cancer Biology Program, The University of Texas Graduate School of Biomedical Sciences at Houston, Houston, Texas.

Note: Supplementary data for this article are available at Molecular Cancer Therapeutics Online (http://mct.aacrjournals.org/).

Corresponding Authors: François X. Claret, Department of Systems Biology, The University of Texas MD Anderson Cancer Center, 7435 Fannin Street, Unit 950, Houston, TX 77054-1901. Phone: 713-563-4204; Fax: 713-563-4205; E-mail: fxclaret@mdanderson.org; and Huiling Yang, Department of Pathophysiology, Zhongshan School of Medicine, Sun Yat-Sen University, Guangzhou, Guangdong 510080, PR China. Phone: 86-20-87332268; Fax: 86-20-87331209; E-mail: hlyangsums@hotmail.com

doi: 10.1158/1535-7163.MCT-14-0317

Of particular interest to us are the genomic loci miR24-1 and miR24-2, which encode the miR24 precursor transcripts pre–miR24-1 (MI0000080, from miRBase, located on chromosome 9q22.32) and pre–miR24-2 (MI0000081, chromosome 19p13.13). Processing of the precursor transcripts by the enzyme Dicer generates three mature miRNAs: miR24-3p (MIMAT0000080) from the 3′ ends of both precursors, and miR24-1-5p (MIMAT0000079) and miR24-2-5p (MIMAT0004497) from the 5′ ends of pre–miR24-1 and pre–miR-24-2, respectively. Many studies have indicated a central regulatory role for miRNAs in the initiation and development of NPC. However, the role of miR24 in NPC or therapy is still unknown.

DNA methylation plays a major role in the transcriptional silencing of certain genes but especially tumor-suppressive genes. Generally, the DNA methylation process is catalyzed by DNA methyltransferases (DNMT), mainly DNMT1 (maintenance DNMT) and DNMT3A and DNMT3B (*de novo* DNMTs), which use *S*-adenosylmethionine as a methyl donor to specifically methylate the fifth carbon atom of the cytosine ring (18). Methylation-mediated silencing of tumor-suppressive genes, genome-wide DNA hypomethylation (which induces chromosomal instability), and spurious gene expression contribute to carcinogenesis (19, 20). miRNAs harboring CpG islands can be directly targeted by DNA hypermethylation (21, 22). Kozaki and colleagues (23) reported that miR199-5b was downregulated in medulloblastomas by methylation of a CpG island 3 kb upstream of the 5′ site of the miR199b-5p promoter, and Vrba and colleagues (24) demonstrated that epigenetic mechanisms are involved in the regulation of miR200c/141 expression in both normal and cancer cells. The fact that the FDA has approved hypomethylating agents such as 5-aza-2′-deoxycytidine for use as anticancer agents indicate the potential for modification of DNA methylation in cancer treatment (25, 26). Although studies have demonstrated the crucial role of DNA methylation in NPC carcinogenesis, the mechanisms by which DNA methylation contributes to NPC radioresistance have yet to be elucidated.

We previously established a radioresistant NPC cell line, CNE-2R, from the parental CNE-2 cell line by high- and gradient-dose IR treatment. These two cell lines differed only in their sensitivity to irradiation but not other cytotoxic agents. We then used qRT-PCR (quantitative real-time PCR) analysis to search for miRNAs differentially expressed between CNE-2 and CNE-2R cells and identified a set of eight miRNAs, including miR24, that were significantly different (27). The objectives of our study were to identify the role of miR24 in NPC tumorigenesis and radioresistance and to identify the mechanisms by which miR24 is regulated. Here, we used qRT-PCR to detect miRNA expression; cytosine-extension assay, methylation DNA immunoprecipitation sequencing (MeDIP-Seq), and methylation-specific PCR (MSP) to measure methylation status; and flow cytometry and Western blotting to assess the cell cycle, apoptosis, and protein expression. Our results support the idea of novel biomarkers for NPC and will facilitate the development of improved therapeutic approaches for patients with NPC.

Materials and Methods

Patient samples

NPC specimens were obtained from patients according to a study protocol approved by the institutional human tissue committee of the Cancer Center of Sun Yat-Sen University in 2011 and 2012. Full, informed consent was obtained from each patient before sample collection. Specimens were obtained by surgical resection and snap-frozen in liquid nitrogen. Primary NPC tumors from patients were diagnosed as NPC before any therapy, and recurrent NPC tumors were diagnosed as NPC reoccurring after radiotherapy. NPC primary and recurrent tissues were matched by sex and similar age. Information about these patients is provided in Supplementary Table S1.

Cell lines and cell culture

Human NPC cell lines: CNE-1 (well differentiated) and CNE-2 (poorly differentiated) were purchased from the Cancer Center of Sun Yat-Sen University, China in 2006, and were not authenticated by us; CNE-2R cells (derived from the parental cell line CNE-2, radioresistant), were established by our group in 2009 (27); and HONE-1 cells (poorly differentiated) were a generous gift 2010 from Prof. Ronald Glaser (Ohio State University Medical Center, Columbus, OH) and were not authenticated by us. All cells were maintained in RPMI-1640 medium (Mediatech, Inc.) containing 10% FBS (Gibco) and 0.5% penicillin–streptomycin sulfate. Cells were stained with trypan blue and counted using the automated cell counter Countess (Invitrogen).

Quantitative real-time PCR

qRT-PCR was used to detect miRNA and H2AX expression. Cells were washed twice in cold PBS (ThermoScientific) before being harvested with TRizol (Ambion). A NanoDrop Lite spectrophotometer (Thermo Scientific) was used to measure the total RNA concentration and purity. For detection of mature miRNA, reverse transcription was performed to convert RNAs to cDNAs using a TaqMan miRNA reverse-transcription kit (Applied Biosystems) and miRNA-specific stem-loop reverse transcription primers by a thermal cycler (Bio-Rad) in one reaction. For H2AX detection, reverse transcription was performed using an ImProm-II transcription system kit (Promega). Finally, PCR reaction mixtures containing TaqMan universal master mix II or SYBR Green PCR master mix (for miRNA and H2AX, respectively) and TaqMan miRNA or gene expression assays (all from Applied Biosystems) were used according to the manufacturer's protocols (gradient S; Mastercycler, Eppendorf) with the software Realplex. Cycling variables were as follows: 50°C for 2 minutes and 95°C for 10 minutes followed by 40 cycles at 95°C (15 seconds) and annealing/extension at 60°C (1

minute). All reactions were performed in triplicate. Data were analyzed with $2^{-\Delta\Delta C_t}$ for relative change in gene expression. U6 snRNA served to normalize miRNA values. GAPDH served to normalize H2AX values.

Colony-formation assay

The colony-formation assay was used to analyze cell growth after treatment with IR or miR24 mimic. NPC cells were plated onto 6- or 12-well plates after irradiation or miR24 mimic transfection. The medium was changed after irradiation for 24 or 48 hours after transfection. After 10 days, cell colonies were fixed with methanol, stained with 0.1% crystal violet, and scored by counting the number of colonies with an inverted microscope, using the standard definition that a colony consists of 50 or more cells. The inhibition ratios of colony formation were calculated as the ratio of the indicated treatment group to the control group: $100\% * N_t/N_c$, where N_t is the colony number of the treatment group and N_c is the colony number of the control group.

miRNA transfection

MirVana miR24 mimics or miRNA inhibitor (Ambion) was transfected into NPC cells to overexpress or inhibit mature miR24-3p. Exponentially growing NPC cells were plated onto 6-well plates using medium without antibiotics 24 hours before transfection. miR24 mimics, miRNA inhibitor, or scramble control (Ambion) was transfected using Lipofectamine 2000 (Invitrogen) as a carrier at a 1:1 ratio.

Flow cytometric analysis of cell cycle and apoptosis

Briefly, NPC cells were collected 48 hours after transfection with miR24 mimic or scramble control. Cells were stained with an Annexin V–FITC apoptosis detection kit I (BD Biosciences) and propidium iodide (PI; Sigma-Aldrich) according to the manufacturer's recommendations. For cell-cycle detection, cells were collected and fixed overnight at −20°C. Samples were measured with a FACScan flow cytometer (Becton Dickinson), and results were analyzed using FlowJo software.

Mouse model

Both flanks of 4- to 6-week-old male BALB/c athymic nu/nu mice were s.c. injected with 50 μL of 1.5×10^6 NPC CNE-2R cells and 50 μL of Matrigel (BD Biosciences). Forty-eight hours later, all mice were transfected with miR-scramble (injected into the left flank) or with miR24 mimic (injected into the right flank) for 48 hours before injection. Tumors were measured on the fifth day after NPC cell injection, when tumors were palpable. Tumors were measured every other day with digital calipers, and tumor volume was calculated using the formula: $mm^3 = (L \times W^2)/2$. Mice were sacrificed on the sixteenth day after injection, when the some of the tumors reached the size limit set by IACUC. Mice were killed by CO_2 asphyxiation, and tumors were weighed after careful resection.

Irradiation

Radiation was performed using a Gammacell 1000 machine (Nordion), a ^{131}I irradiator at The University of Texas MD Anderson Cancer Center (Houston, TX). Cells were suspended in cell medium before irradiation. The irradiation rate was 283 rads/min.

Cell proliferation assay

The cell proliferation assay was used to evaluate cell viability with thiazolyl blue tetrazolium bromide (MTT; Sigma-Aldrich). Briefly, NPC cells were seeded into 96-well plates after irradiation in 200 μL of RPMI-1640. For 5-aza-2′-deoxycytidine treatment, cells were plated into 96-well plates 24 hours before 5-aza-2′-deoxycytidine was added. After the indicated incubation period, MTT (5 mg/mL) was added, the cells were incubated at 37°C for 24 hours, and 10 μL of the solubilization reagent 10% SDS was added to each well. Spectrophotometric absorbance of the samples was measured at 570 nm with a microplate reader (Molecular Devices) after an additional 4 hours of incubation. The inhibition ratios of cell survival were calculated as: $100\% * N_t/N_c$, where N_t is the optical density of the treatment group and N_c is the optical density of the control group.

Cytosine-extension assay

Cytosine-extension assay was performed to detect genome-wide methylation status as previously described by Pogribny and colleagues (28). Briefly, genomic DNA was pretreated with *Hpa*II (New England Biolabs) following the manufacturer's protocol. A second DNA aliquot incubated without restriction enzyme served as the background control. The single-nucleotide extension reaction was performed in a 25-μL reaction mixture containing 0.25 μg of DNA, 1× PCR buffer II, 1.0 mmol/L $MgCl_2$, 0.25 U of AmpliTaq DNA polymerase (PerkinElmer), and 57.4 Ci/mmol/L [^{3}H]dCTP (DuPont NEN) and incubated at 56°C for 1 hour. Results are displayed as the percentage change from control samples.

Methylated DNA immunoprecipitation sequencing

MeDIP-Seq was performed to compare alterations in the DNA methylation patterns in the CNE-2 and CNE-2R cell lines. Jacinto and colleagues (29) first reported this method for mapping methylation profiles to better understand the implications of methylation changes in the regulation of gene expression. Briefly, DNA was fragmented by ultrasonic waves, modified at the 3′ terminal end by adding adenine using an Illumina paired-end DNA sample prep kit, and then denatured. The 5-methylcytosine antibody was then added for immunoprecipitation using a Diagenode magnetic methylated DNA immunoprecipitation kit to enrich methylated DNA fragments, which was followed up with high-throughput sequencing. Data were ultimately analyzed using standard bioinformatic analysis, which was performed for comparison with the personalized analysis (30). In brief, sequencing data were filtered to get clean data, followed by a comparative

analysis. The unique mapped reads (by an alignment analysis between MeDIP-seq data and the reference genome) were used to analyze the genome and the distribution of gene elements. A comparison analysis was performed for the peak coverage at different gene elements to identify the differentiated genes between two samples ($P \leq 0.05$), followed by the Go and Pathway analyses (31).

Methylation-specific PCR

MSP was performed to analyze the methylation of the miR24-1 promoter in NPC cells with or without irradiation. Briefly, DNA samples were extracted with a PureLink genomic DNA mini kit (Invitrogen), converted with an EpiTect bisulfite kit (Qiagen) following the manufacturer's protocol, and amplified by PCR using methylated and unmethylated specific primers for miR24-1. By bisulfite conversion, nonmethylated cytosines were transformed into uracils and methylated cytosines remained unconverted. PCR products were subsequently electrophoresed by 1.5% agarose gel stained with GelRed nucleic acid (Biotium) and finally exposed to UV radiation.

Two sets of miR24-1 primers were designed with MethPrimer software (32): left methylated primer, ATTATGTGTTAGGAAAGGGAAAC; right methylated primer, CTATATACCGCCAACCCGTC; left unmethylated primer, ATTATGTGTTTAGGAAAGGGAAAT; and right unmethylated primer, ACAATCTATATACCACCAACCCATC.

Experiment with 5-aza-2′-deoxcycytidine

The DNA-hypomethylating drug 5-aza-2′-deoxycytidine (Sigma-Aldrich) was used to verify the DNA methylation regulation of NPC cells. Briefly, NPC cells were plated onto 60-mm dishes or 96-well plates 24 hours before treatment with 5-aza-2′-deoxcycytidine. Acetic acid (50%) was used to dissolve the 5-aza-2′-deoxcycytidine, and the control group was treated with the same amount of 50% acetic acid as the 10 μmol/L 5-aza-2′-deoxcycytidine. RNA was isolated 96 hours after treatment with 5-aza-2′-deoxcycytidine to examine miR24 and H2AX expression.

Statistical analysis

Statistical analysis was performed using SPSS statistical software (Chicago). Data are presented as the mean ± SD. Statistical analyses were performed by one-way ANOVA when there were more than two groups. The Student *t* test was used when there were only two groups. The statistical significance level was set as $P = 0.05$ (two-sided). Differences between groups were considered to be significant statistically when $P \leq 0.05$.

Results

miR24 is involved in NPC radioresistance

The radioresistant NPC cell line CNE-2R was established with an escalating dose of IR over 12 months from the parental cell line CNE-2 (Supplementary Fig. S1A) before this study was initiated. We used microarray and qRT-PCR analyses to search for miRNAs differentially expressed in CNE-2 and CNE-2R cells (Supplementary Fig. S1B). We identified 14 miRNAs whose expression differed by a factor of two or more ($P < 0.01$) between the two cell lines and designated the gene set as the radioresistant miRNA signature (Supplementary Table S2). qRT-PCR was performed to verify miRNA expression, and eight of the 14 miRNAs were identified to be significantly altered, where five miRNAs were downregulated (miR24, miR18a, miR19b, miR93, and miR103) and three miRNAs were upregulated (miR205, miR224, and let 7g) in CNE-2R cells (Supplementary Fig. S1C; ref. 27).

We next measured the expression levels of these eight miRNAs in six pairs of matched NPC patient samples. As shown in Fig. 1A (heat map) and 1B (bar graph), of all six pairs, only mature miR24 had consistently reduced expression (around 50%) in recurrent NPC tissues compared with primary NPC tissues. Therefore, we focused on investigating the potential role of miR24 in regulating the sensitivity of NPC to IR.

To investigate the involvement of miR24 in NPC radioresistance, we first examined the radiosensitivity of the NPC cell lines. As expected, after 24 hours of exposure to 4 Gy, the CNE-2R cell line maintained relative radioresistance: It retained 27% of its colonies whereas the CNE-2 cell line had only 3% of its colonies (Fig. 1C). Interestingly, the HONE-1 cell line displayed a radioresistant phenotype compared with the CNE-1 cell line (Fig. 1C). qRT-PCR demonstrated that the miR24 expression level was more than 50% lower in the NPC radioresistant CNE-2R and HONE-1 cells than in the CNE-2 and CNE-1 cells, respectively (Fig. 1D). Our findings showed that miR24 was downregulated both in recurrent NPC tissue samples and in relatively radioresistant NPC cells, implicating miR24 in NPC radioresistance.

miR24 suppresses cell growth *in vitro* and reduces tumor growth in mouse models

Because miR24 expression correlated positively with NPC radiosensitivity, we next investigated the role of miR24 in NPC by overexpressing miR24 using miR24 mimics (Fig. 2A). NPC cells transfected with miR24 mimics exhibited significant cell growth inhibition. Cell survival was greatly inhibited in all four NPC cell lines (CNE-2, CNE-2R, CNE-1, and HONE-1; Fig. 2B). The relatively radioresistant cell lines CNE-2R and HONE-1 were much more inhibited than the CNE-2 and CNE-1 cell lines, respectively. We used the clonogenic assay to evaluate the oncogenic potential of this miRNA. Colony-formation ability was significantly suppressed in NPC cells by overexpression of miR24; CNE-2R cells in particular were completely suppressed with 30 nmol/L miR24 mimic (Fig. 2C). Interestingly, both cell survival and clonogenic assay results revealed that the CNE-2R cell line was the most sensitive to miR24 overexpression.

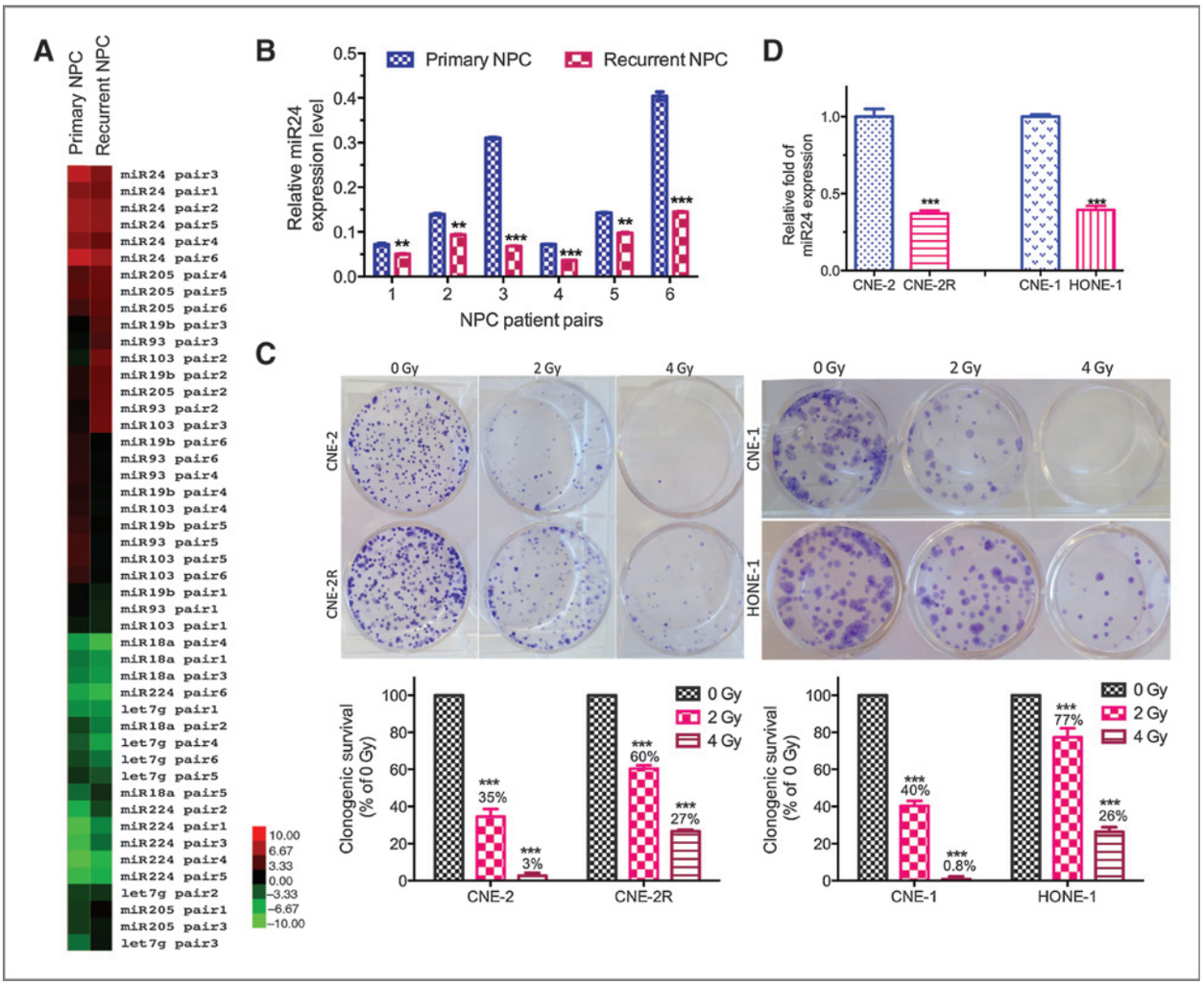

Figure 1. miR24 expression is positively correlated with the sensitivity of NPC to IR. A, miRNA signature in NPC tissues. Heatmap of eight miRNAs expressed differentially in six pairs of matched NPC primary and recurrent tissues. Lowest expression is represented by green and highest expression by red. Data were normalized to the median value by $\log_2$ before mapping using software programs Cluster and TreeView. B, bar graphs of miR24 differential expression levels between the six pairs of matched NPC recurrent tissues compared with primary tissues, as determined by qRT-PCR. Raw data were analyzed with $2^{-\Delta\Delta C_t}$. U6 snRNA was used as an internal control. C, characterization of NPC cell lines. CNE-2, CNE-2R, CNE-1, and HONE-1 cells were exposed to IR (0, 2, or 4 Gy) and colony-formation assay was measured at 24 hours. In a dose-dependent manner, CNE-2R cells were more resistant to radiation than CNE-2 cells (left) and HONE-1 cells were more resistant than CNE-1 cells (right). The colony ratio (%) is relative to 0 Gy. Data, mean ± SD of three independent experiments. D, relative miR24 expression levels of NPC radioresistant cell lines (CNE-2R and HONE-1) compared with radiosensitive cell lines (CNE-2 and CNE-1) as determined by qRT-PCR. miR24 expression levels in CNE-2R and HONE-1 cells were normalized to those of CNE-2 and CNE-1 cells, respectively. Data, mean ± SD of three independent experiments; **, $P < 0.01$; ***, $P < 0.001$.

Using flow cytometry, we next measured the rate of cell apoptosis in NPC cells overexpressing miR24. A significant induction of apoptosis was observed in both the early and late stages in a dose-dependent manner in all NPC cells transfected with miR24 mimics (Fig. 2D). Consistently, cell apoptosis was induced the most in CNE-2R cells, indicating the best response of CNE-2R to miR24 overexpression. Cells were then stained with only PI for measuring the percentage of sub-G_1 cells (Fig. 2E). A significant increase ($P < 0.0001$) in sub-G_1 cells was observed in all NPC cell lines (data not shown for CNE-2 and CNE-1 cells).

To confirm the role of miR24 in suppressing cell growth *in vivo*, the miR24 stably expressing NPC CNE-2R cells and the miR-scramble vector (control) were s.c. injected into the right and left flanks of mice, respectively. On days 12 and 16, the mean size of the tumors from mice injected with miR24-expressing cells was significantly smaller (67% and 74%, respectively) than that of mice injected with miR-scramble (Fig. 2F). Taken together, the data suggested that miR24 expression of NPC CNE-2R cells is associated with tumor reduction. We found that miR24 inhibited the growth of NPC cancer cell xenografts. Taken together, these

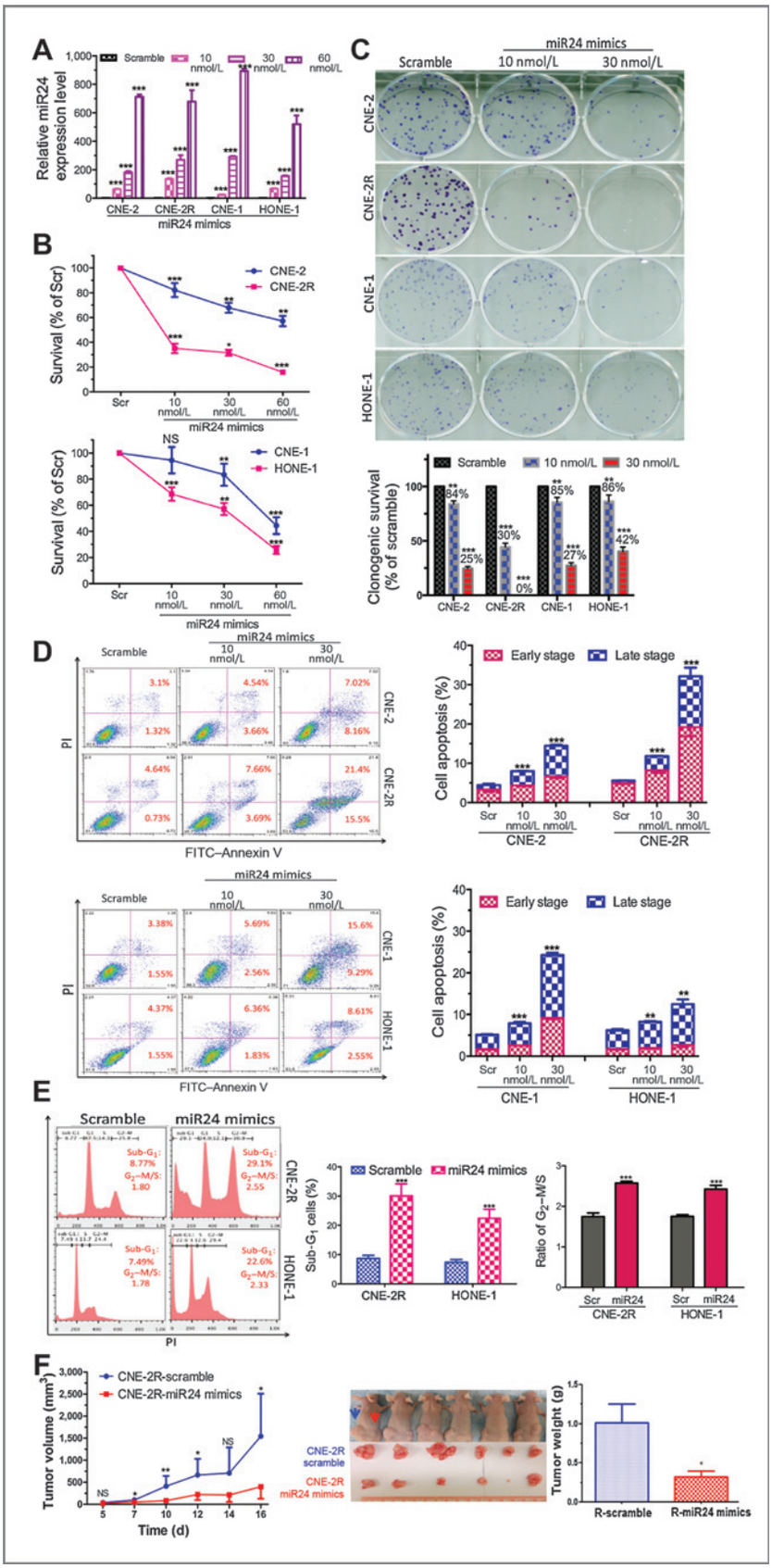

Figure 2. miR24 functions as a growth inhibitory factor in NPC cells and xenografts. A, verification by qRT-PCR of miR24 expression after transfection with miR24 mimic (10, 30, or 60 nmol/L) or control (scramble, Scr) for 48 hours. Data, mean ± SD of three independent experiments. B, cell numbers were determined with an automated cell counter 48 hours after transfection with miR24 mimic (10, 30, or 60 nmol/L). Data are normalized to Scr and represent mean ± SD of three independent experiments. C, effects of overexpression of miR24 on the clonogenic ability of CNE-2, CNE-2R, CNE-1, and HONE-1 cells. Representative examples of colony-formation assays in CNE-1, HONE-1, CNE-2, and CNE-2R cells (top). The percentage of colonies treated with miR24 mimic (10 or 30 nmol/L) relative to colonies treated with scramble control (bottom). Data, mean ± SD of three independent experiments. D, representative results of cell apoptosis assay by flow cytometry in NPC cells (left). Red numbers, percentages of apoptosis. Quantification of the percentage of apoptotic cells (right) is shown. Data, mean ± SD of three independent experiments. E, representative results of flow cytometry with PI staining after transfection with 30 nmol/L miR24 mimic and scramble control (left). Sub-G_1 cell percentages and G_2–M/S ratios are shown in red. Bar charts, the percentage of sub-G_1 cells (middle) and the ratio of G_2–M/S cells (right) in CNE-2R and HONE-1 cells. Data, mean ± SD of three independent experiments; ***, $P < 0.001$ versus scramble. F, miR24 suppresses tumor growth of NPC xenografts. *In vivo* experiment illustrating the injection of radioresistant NPC (CNE-2R) cells stably expressing miR24 or miR-scramble into nude mice. Tumor size is reported as mean tumor volume ± SD for each group of 6 mice (left). Mice with tumors and resected tumors are shown in middle. Red arrow, miR24-overexpressing group injected in right flank. Blue arrow, miR-scramble group injected in left flank. Bar graph, tumor weight of the two treatment groups (right); NS, not significant; *, $P < 0.05$; **, $P < 0.001$; ***, $P < 0.0001$.

results indicate a potential tumor-suppressive role for miR24 in NPC cells.

miR24 is a potential radiosensitizor in NPC cells

Considering the role of miR24 in NPC cells and the involvement of miR24 in NPC radioresistance, we hypothesized that miR24 can alter cellular sensitivity to IR in NPC. The cell cycle is a critical process during radiotherapy. Cells in the G_2–M phase tend to be the most sensitive to irradiation among all the cell-cycle phases, whereas cells in the S phase tend to resist irradiation the most. Figure 2E showed a significant increase in the ratio of G_2–M phase to S phase in HONE-1 and CNE-2R miR24-treated cells than in cells treated with control scramble miR (ratios, 2.3 and 2.5 vs. 1.7 and 1.8, respectively; $P < 0.001$ for each cell line).

As was shown in Fig. 2C, CNE-2 and HONE-1 cells were less sensitive to miR24 overexpression than were CNE-2R and CNE-1 cells, respectively. To determine the role of miR24 under IR, we combined IR with miR24 mimics to reassess colony formation. Our results showed that colony formation dropped from 84% to 18% in CNE-2 cells and from 86% to 14% in HONE-1 cells when treated with 2 Gy IR compared with scramble groups (Fig. 3A).

Moreover, in miR24-overexpressing cells, compared with no IR, 10-Gy IR increased the rate of cell apoptosis from 1.24- to 2.10-fold in CNE-2R cells, from 1.17- to 1.45-fold in HONE-1 cells, from 1.48- to 1.77-fold in CNE-2

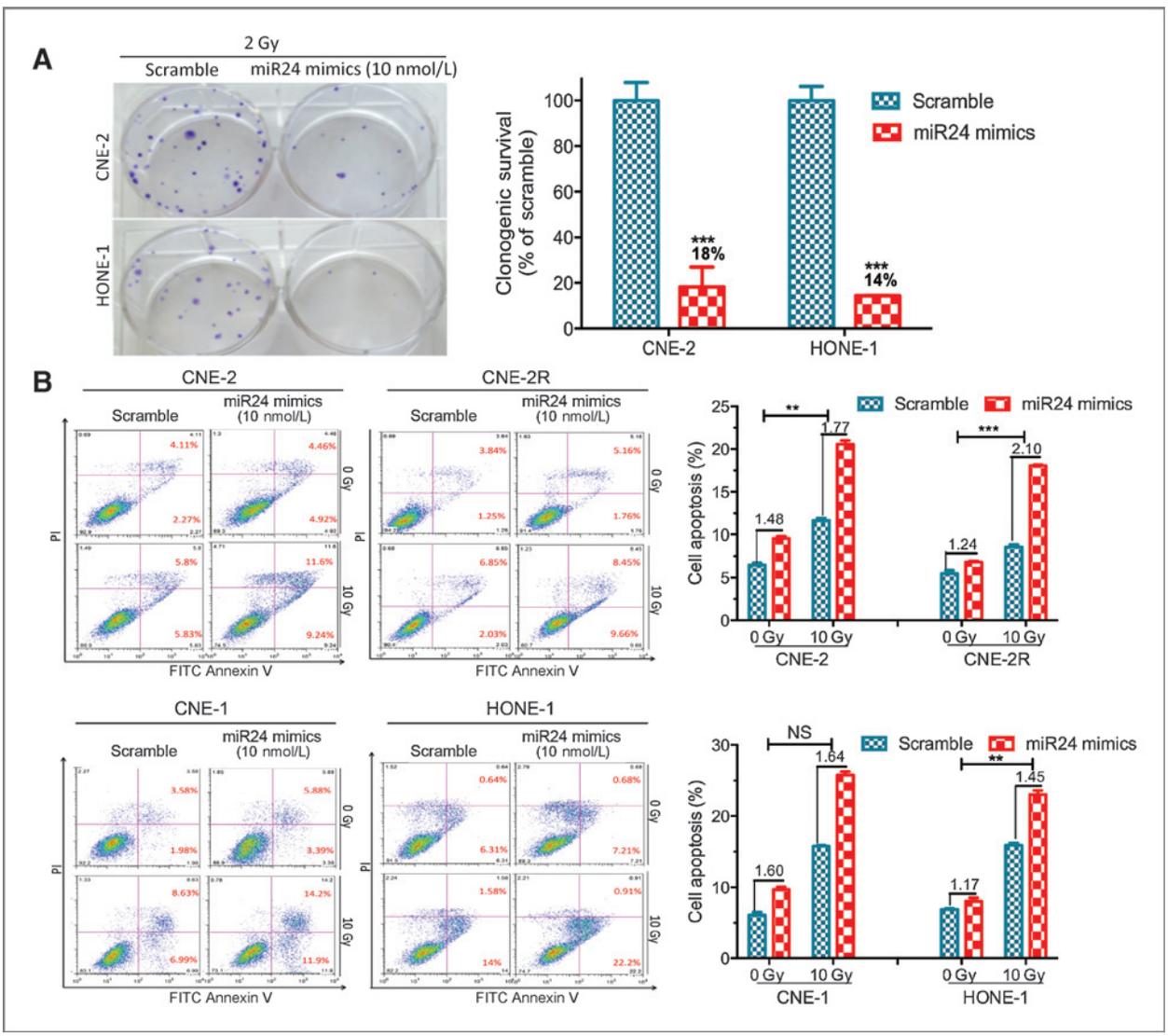

Figure 3. miR24 increases radiosensitivity of NPC cells. A, representative colony-formation assay results following transfection with miR24 mimics (10 nmol/L) or scramble control and combined with 2-Gy irradiation treatments. Data, mean ± SD of three experiments. B, representative results of cell apoptosis assay by flow cytometry stained with PI and FITC–Annexin V (left). Apoptosis percentages appear in red. Quantification of apoptotic cells shows the fold of miR24 mimics (10 nmol/L) to the control group (right). Data, mean ± SD of at least three independent experiments; NS, not significant; **, $P < 0.001$; ***, $P < 0.0001$.

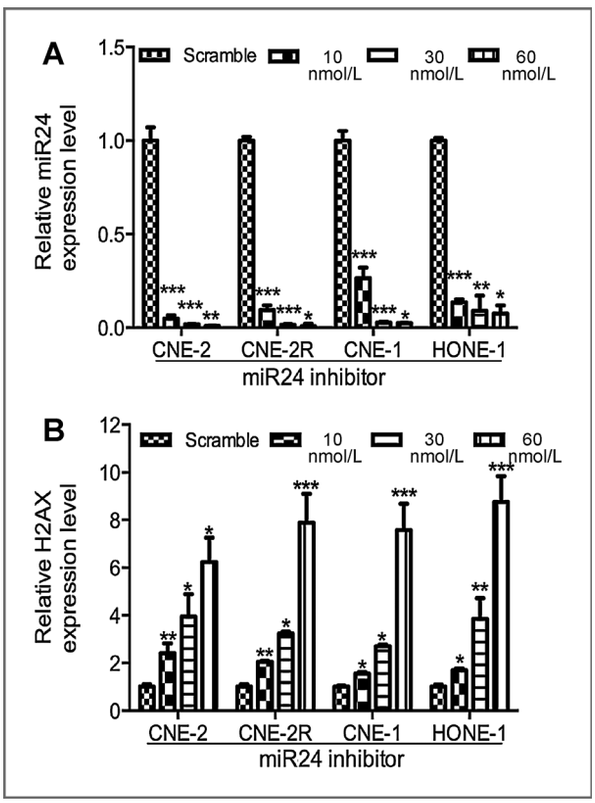

Figure 4. Loss of miR24 impairs cell apoptosis and promotes DNA-damage repair. A, miR24 expression levels as determined by qRT-PCR following transfection with an miR24 inhibitor (10, 30, or 60 nmol/L) or scramble-miR (10 nmol/L) as a control in NPC cells for 48 hours. Data, mean ± SD of three independent experiments. B, qRT-PCR results of H2AX expression at mRNA levels by transfecting with an miR24 inhibitor (10, 30, or 60 nmol/L) or scramble control (10 nmol/L). GAPDH served as an internal control. Data, mean ± SD of three independent experiments; *, $P < 0.05$; **, $P < 0.001$; ***, $P < 0.0001$.

cells, and from 1.60- to 1.64-fold in CNE-1 cells (Fig. 3B). These data indicate that, compared with the radiosensitive cell lines (CNE-2 and CNE-1), the radioresistant cell lines (CNE-2R and HONE-1) exhibit higher sensitivity under IR treatment when combined with miR24 mimics. These data demonstrated that miR24 could sensitize NPC cells to IR treatment.

Inhibition of miR24 expression increases H2AX in NPC cells

To reveal how miR24 functions in NPC, we inhibited its endogenous expression using an miR24 inhibitor. qRT-PCR revealed that the miR24 level was remarkably decreased in all four NPC cell lines, as we expected (Fig. 4A). The histone variant H2AX is a key double-strand break (DSB) repair protein that has been proven to be a target of miR24 in HepG2 cells (33). They demonstrated that miR24 upregulation reduces H2AX, and thereby renders them vulnerable to DNA damage. Consistent with their results, in our NPC model, H2AX was upregulated in a dose-dependent manner upon miR24 inhibition with increasing doses of the miR24 inhibitor in all four NPC cells (Fig. 4B). This finding indicates a possible mechanism by which miR24 is involved in the response to radiotherapy of NPC cells, strongly supporting our hypothesis that miR24 is crucial in NPC radioresistance.

Hypermethylation of mir24-1 contributes to NPC radioresistance

It is well documented that radiation can induce global genome DNA hypomethylation, leading to genome instability (34). However, the role of methylation in NPC radioresistance is still unknown. Thus, we evaluated whether differences in DNA methylation could be observed between CNE-2 and CNE-2R cells. The genome-wide methylation level was approximately 30% lower in CNE-2R cells than in CNE-2 cells (Supplementary Fig. S2), indicating that DNA methylation is indeed involved in NPC radioresistance.

To confirm the role of DNA methylation in NPC radioresistance, we next used MeDIP-Seq to analyze the methylation pattern of CNE-2 and CNE-2R cells. Our data showed that the methylation pattern of hundreds of genes had altered at the gene function elements, including the upstream 2K sequence, 5′UTR, coding sequence, intron, 3′UTR, and downstream 2K sequence (Supplementary Fig. S3A and Supplementary Table S3). We next analyzed the gene methylation patterns that differed between the two cell lines by Go and Pathway analysis. We found that these genes were involved in almost all biologic functions, including biologic processes, cellular components, and molecular functions (Supplementary Fig. S3B). To be more specific, genes involved mainly in biologic regulation, cellular processes, metabolic processes, cell parts, and molecular binding were dysregulated in DNA methylation patterns. Clearly, altered DNA methylation is associated with NPC radioresistance.

Because both DNA methylation and miR24 appear to be associated with NPC radioresistance, we hypothesized that loss of miR24 in recurrent NPC is regulated by DNA methylation. Mature miR24-3p is cleaved from its precursor miR24-1 and miR24-2, which are located at chromosomes 9q22.32 and 13.13, respectively; only miR24-1 was embedded in a CpG island (Supplementary Fig. S4). We used MethPrimer software to analyze the CpG island area of the 2K upstream sequence of the miR24-1 promoter. From this analysis, we designed the primers for methylation detection in the region of the miR24-1 promoter by MSP.

Methylation status was measured in the two pairs of radioresistant and radiosensitive cell lines (CNE-2 and CNE-2R; CNE-1 and HONE-1). Interestingly, the miR24-1 promoter was hypermethylated in both radioresistant cell lines (CNE-2R and HONE-1) compared with the corresponding radiosensitive cell lines (CNE-2 and CNE-1, respectively; Fig. 5A). Combined with our previous data shown in Fig. 1D, this finding revealed an inverse correlation between miR24-1 promoter methylation status and mature miR24 expression. We next measured the

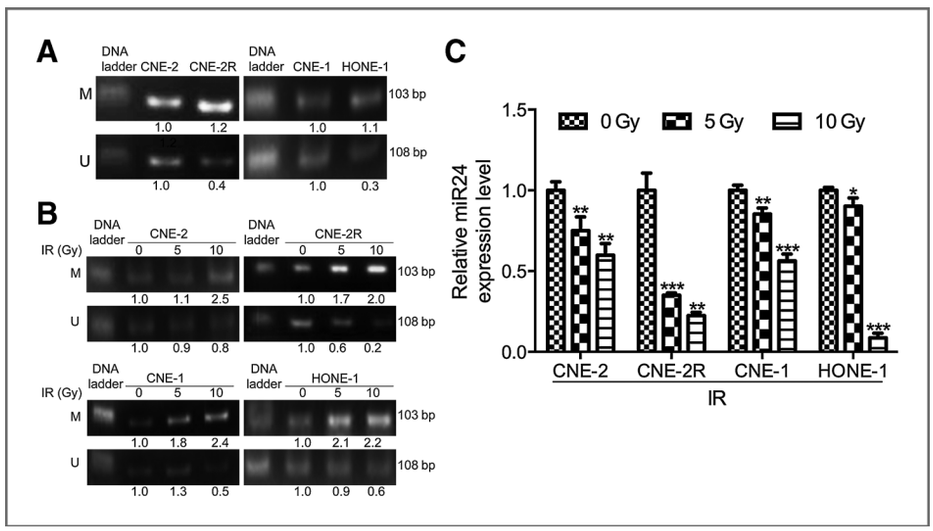

Figure 5. Promoter of miR24-1 is hypermethylated in NPC radioresistant cells. A, representative MSP results of methylation status of the mir24-1 promoter in NPC cell lines. M, methylated primers; U, unmethylated primers. B, representative MSP results of the mir24-1 promoter methylation status after IR (0, 5, or 10 Gy) treatment in NPC cells are shown. Data were quantified by ImageJ software. C, qRT-PCR results of miR24 expression after IR treatment (0, 5, or 10 Gy) for 24 hours are shown. Data, mean ± SD of three independent experiments; *, $P < 0.05$; **, $P < 0.001$; ***, $P < 0.0001$.

methylation status of the miR24-1 promoter and found that it was hypermethylated after IR treatment in a dose-dependent manner in all four NPC cell lines (Fig. 5B). These findings suggested that hypermethylation of the miR24-1 promoter is associated with the response of NPC cells to IR. In addition, a decrease level of miR24 expression was measured under IR treatment in a dose-dependent manner (Fig. 5C), conforming the inverse correlation between miR24-1 promoter methylation status and miR24 expression under IR treatment.

5-Aza-2′-deoxycytidine treatment can increase miR24 expression in NPC cells

As we noted, mature miR24 was inversely correlated with the methylation status of the miR24-1 promoter, and this promoter was significantly hypermethylated after IR treatment. To better determine the regulation of miR24 by DNA methylation, we used 5-aza-2′-deoxycytidine to analyze the effect of demethylation on miR24. The reduced miR24 expression was compensated for by hypomethylation in a dose-dependent manner, which provided solid evidence that miR24 inhibition could be regulated by hypermethylation of its promoter (Fig. 6A). Furthermore, inhibition of H2AX expression and NPC cell growth was observed after 5-aza-2′-deoxycytidine treatment and miR24 compensation, which was consistent with the role of DNA-damage repair in miR24-mediated function in NPC (Fig. 6B) and the role of miR24 as a tumor-suppressive factor in NPC (Fig. 6C). These findings indicated the regulation of miR24 by hypermethylation of the miR24-1 promoter in NPC.

Discussion

Recent demonstrations of differential expression of miRNAs in cancer and the function of some miRNAs as oncogenes (called "oncomiRs") or tumor-suppressive genes ("tumor-suppressive miRNAs") have spurred considerable interest in the elucidation of their roles in cancer. miR24, an abundant miRNA that is well conserved among species, has attracted much attention due to its important role in various biologic and pathologic processes, including cell proliferation, cell cycle, apoptosis, and differentiation. It is expressed in normal tissues such as adipose tissue, mammary gland, kidney, and differentiated skeletal muscles (35); however, it is dysregulated in cancer. Lin and colleagues (36) reported that miR24 was upregulated in oral SCC tissues, plasma, and cell lines in comparison with their normal counterparts, whereas Wu and colleagues (37) found that miR24 was downregulated in gastric cancer cells, indicating a dual role for miR24 in cancers. Indeed, the same miRNA can have different functions in different cancers. For example, miR24 promotes the proliferation of HuH7 hepatocellular carcinoma cells as well as A549 lung carcinoma cells but inhibits HeLa cell proliferation (38), perhaps because the targets of miR24 differ by cancer type.

Our findings established, for the first time, that miR24 functions as a tumor-suppressor miRNA in NPC by inhibiting cell proliferation and promoting apoptosis, which is consistent with the studies of Lal and colleagues (39) and Mishra and colleagues (40). In addition, we discovered that miR24 expression was decreased in both NPC radioresistant cells and recurrent NPC tissue samples, which suggested the involvement of miR24 in NPC radioresistance. To identify the role of miR24 in the effect of radiotherapy on NPC, we combined IR treatment with enhanced miR24 expression and found that miR24 radiosensitized NPC cells.

IR produces intermediate ions and free radicals that induce cell inactivation and cell death mainly through inflicting DNA DSBs. Nonhomologous end-joining is the major DNA repair pathway involved in the repair of DSBs after IR (41). The histone variant H2AX is a critical molecule in the response to DSB and leads to DNA repair; H2AX is also a known target of miR24 (33). Thus, overexpressing miR24 is expected to increase cell sensitivity to IR, which is one probable way that miR24 acts as a

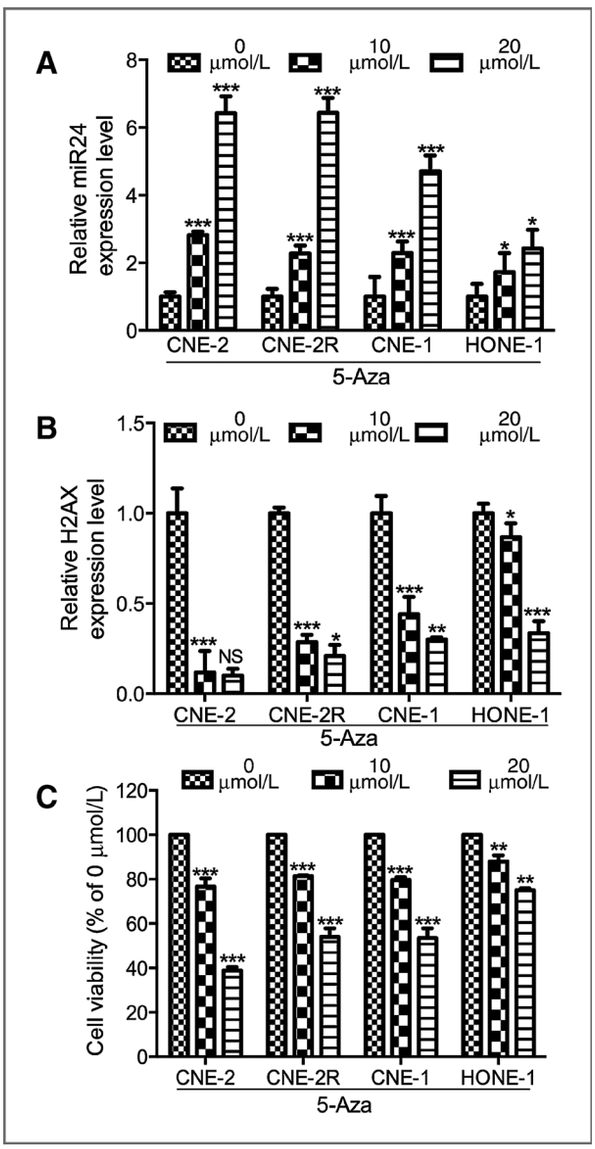

Figure 6. Increased miR24 expression and inhibition of H2AX levels following 5-aza-2′-deoxycytidine treatment (0, 10, or 20 μmol/L) for 96 hours. A, qRT-PCR results of miR24 expression after 5-aza-2′-deoxycytidine treatment are shown. Data, mean ± SD of three independent experiments. B, qRT-PCR results of H2AX expression after 5-aza-2′deoxycytidine treatment are shown. Data, mean ± SD of three independent experiments. GAPDH served as an internal control. C, MTT assay results of NPC cell viability after treatment. Cell viability percentages are normalized to 0 μmol/L. Data, mean ± SD of three independent experiments. NS, not significant; *, $P < 0.05$; **, $P < 0.001$; ***, $P < 0.0001$.

radiosensitizer in NPC. We assessed H2AX expression with miR24 inhibitors in the four NPC cell lines and discovered, as expected, that H2AX increased markedly after miR24 inhibition in all four NPC cell lines. All together, our data indicated that DNA-damage repair, cell apoptosis, and cell-cycle manipulation are all conceivable processes by which miR24 modulates response to NPC radiotherapy.

Global hypomethylation and aberrant hypermethylation of gene promoter CpG islands result in tumor cell genomic instability and gene silencing (particularly of tumor-suppressive genes), respectively (42). During the last decade, the appearance of cancer-specific upstream region hypermethylation of miRNAs has been demonstrated to be an epigenetic mechanism for aberrant miRNA expression (15, 43). Numerous reports have documented the mutual regulation between ectopic miRNA expression and aberrant DNA methylation, which was first confirmed in cancer research.

miRNA-encoding genes are both targets and regulators of methylation. On the one hand, ectopic miRNA expression could be regulated by DNA methylation primarily via hypermethylation of the promoter region of the miRNA gene (usually pointing to tumor-suppressive miRNAs). For instance, miR342 inhibition in colorectal cancer could be mediated epigenetically by hypermethylation of its promoter (44). Another study reported that the DNA methylation inhibitor 5-aza-2′-deoxycytidine could induce miR127 expression in cancer cells, confirming that miRNA can be targeted by DNA methylation (45). On the other hand, aberrant methylation could be manipulated by miRNA primarily through targeting DNA methyltransferases or DNA methylation-related proteins. miR29 (miR29-a, -b, or -c; also called "epi-miRNAs") can reverse aberrant methylation in lung cancer by targeting DNMT3A and DNMT3B (18). Chen and colleagues (46) reported that miR373 could negatively regulate methyl-CpG–binding domain protein 2 directly in cholangiocarcinoma.

In our present study, we measured the genome-wide methylation level between CNE-2 and CNE-2R cells and showed that DNA methylation was approximately 30% lower in CNE-2R cells, indicating genomic instability after irradiation by DNA methylation alteration. We searched miR24 genes and found that only miR24-1 was embedded in CpG islands. MSP was subsequently performed to test the methylation level of the miR24-1 promoter, and the results revealed hypermethylation in both radioresistant NPC cells and NPC cells after IR treatment. In addition, miR24 was downregulated after irradiation, which was adversely correlated with the methylation status of its promoter. Furthermore, 5-aza-2′-deoxycytidine reversed the hypermethylation pattern and compensated for the miR24 inhibition. Taken together, our findings suggested that the mechanism by which miR24 mediates NPC radioresistance is regulated epigenetically by mir24-1 promoter hypermethylation.

Epigenetic modifications, particularly miRNAs and DNA methylation, have been gaining more and more attention due to their potential as therapeutic targets. First, miRNAs are very stable, even in body fluids such as plasma, serum, urine, and saliva (47). Second, miRNAs have multiple functions and are involved in almost every physiologic and pathologic process, and thus clearly have crucial roles and potentially profound effects in cancer

treatment. Third, cancer-specific miRNA signatures can be highly reproducible and independently predictive of clinical and biologic features of tumors, and thus very useful in improving treatment (48). Lu and colleagues (49) successfully inhibited the tumorigenicity of NPC cells in nude mice *in vivo* by using lenti-miR26a as gene therapy. Moreover, the first miRNA-targeted drug, miravirsen, a locked nucleic acid-modified oligonucleotide, has gone through preclinical trials with primates (50). Miravirsen has also been determined to be safe and well tolerated and to result in a significant dose-dependent decrease in hepatitis C RNA levels in patients (51). In addition, some demethylating agents have been approved by the FDA as anticancer drugs. In conclusion, we have provided new insight into NPC treatment. Our findings defined a central role for miR24 as a potential tumor-suppressor miRNA in NPC and they suggested a use for miR24 in novel therapeutic strategies to treat this cancer.

Disclosure of Potential Conflicts of Interest

No potential conflicts of interest were disclosed.

Authors' Contributions

Conception and design: S. Wang, F.X. Claret, H. Yang
Development of methodology: S. Wang, F.X. Claret
Acquisition of data (provided animals, acquired and managed patients, provided facilities, etc.): S. Wang, R. Zhang, F.X. Claret, H. Yang
Analysis and interpretation of data (e.g., statistical analysis, biostatistics, computational analysis): S. Wang, F.X. Claret
Writing, review, and/or revision of the manuscript: S. Wang, F.X. Claret
Administrative, technical, or material support (i.e., reporting or organizing data, constructing databases): S. Wang, F.X. Claret, H. Yang
Study supervision: F.X. Claret, H. Yang

Acknowledgments

The authors thank Elizabeth L. Hess in the Department of Scientific Publications at MD Anderson for editing the article.

Grant Support

This work was supported by a fellowship from the China Scholarship Council (201206380043; to S. Wang), the National Natural Science Foundation of China (81071837, 81372410, and 30670627; to H. Yang), the Scientific and Technological Project of Guangdong, China (2008A030201009 and 2010B050700016; to H. Yang), and grants from the National Cancer Institute (R01-CA90853; to F.X. Claret), the Sister Institution Network Fund (to F.X. Claret), and The University of Texas MD Anderson Functional Proteomics Core Facility (NCI Cancer Center Support Grant CA16672).

The costs of publication of this article were defrayed in part by the payment of page charges. This article must therefore be hereby marked *advertisement* in accordance with 18 U.S.C. Section 1734 solely to indicate this fact.

Received April 10, 2014; revised August 27, 2014; accepted October 6, 2014; published OnlineFirst October 15, 2014.

References

1. Lo KW, Chung GT, To KF. Deciphering the molecular genetic basis of NPC through molecular, cytogenetic, and epigenetic approaches. Semin Cancer Biol 2012;22:79–86.
2. Wei WI, Sham JS. Nasopharyngeal carcinoma. Lancet 2005;365:2041–54.
3. Lee FK, Yeung DK, King AD, Leung SF, Ahuja A. Segmentation of nasopharyngeal carcinoma (NPC) lesions in MR images. Int J Radiat Oncol Biol Phys 2005;61:608–20.
4. Chan AT. Nasopharyngeal carcinoma. Ann Oncol 2010;21 Suppl 7:vii308–12.
5. Chen HC, Chen GH, Chen YH, Liao WL, Liu CY, Chang KP, et al. MicroRNA deregulation and pathway alterations in nasopharyngeal carcinoma. Br J Cancer 2009;100:1002–11.
6. Liu S, Dontu G, Mantle ID, Patel S, Ahn NS, Jackson KW, et al. Hedgehog signaling and Bmi-1 regulate self-renewal of normal and malignant human mammary stem cells. Cancer Res 2006;66:6063–71.
7. Chan MC, Hilyard AC, Wu C, Davis BN, Hill NS, Lal A, et al. Molecular basis for antagonism between PDGF and the TGFbeta family of signalling pathways by control of miR-24 expression. EMBO J 2010;29:559–73.
8. Claret FX, Hibi M, Dhut S, Toda T, Karin M. A new group of conserved coactivators that increase the specificity of AP-1 transcription factors. Nature 1996;383:453–7.
9. Calin GA, Croce CM. MicroRNA signatures in human cancers. Nat Rev Cancer 2006;6:857–66.
10. Bounpheng MA, Melnikova IN, Dodds SG, Chen H, Copeland NG, Gilbert DJ, et al. Characterization of the mouse JAB1 cDNA and protein. Gene 2000;242:41–50.
11. Tian L, Peng G, Parant JM, Leventaki V, Drakos E, Zhang Q, et al. Essential roles of Jab1 in cell survival, spontaneous DNA damage and DNA repair. Oncogene 2010;29:6125–37.
12. He ML, Luo MX, Lin MC, Kung HF. MicroRNAs: potential diagnostic markers and therapeutic targets for EBV-associated nasopharyngeal carcinoma. Biochim Biophys Acta 2012;1825:1–10.
13. Lee RC, Feinbaum RL, Ambros V. The C. elegans heterochronic gene lin-4 encodes small RNAs with antisense complementarity to lin-14. Cell 1993;75:843–54.
14. Bartel DP. MicroRNAs: genomics, biogenesis, mechanism, and function. Cell 2004;116:281–97.
15. Calin GA, Croce CM. MicroRNA-cancer connection: the beginning of a new tale. Cancer Res 2006;66:7390–4.
16. Almeida MI, Reis RM, Calin GA. Decoy activity through microRNAs: the therapeutic implications. Expert Opin Biol Th 2012;12:1153–9.
17. Kamanu TKK, Radovanovic A, Archer JAC, Bajic VB. Exploration of miRNA families for hypotheses generation. Sci Rep-Uk 2013;3:2940.
18. Fabbri M, Garzon R, Cimmino A, Liu Z, Zanesi N, Callegari E, et al. MicroRNA-29 family reverts aberrant methylation in lung cancer by targeting DNA methyltransferases 3A and 3B. Proc Natl Acad Sci U S A 2007;104:15805–10.
19. Datta J, Kutay H, Nasser MW, Nuovo GJ, Wang B, Majumder S, et al. Methylation mediated silencing of microRNA-1 gene and its role in hepatocellular carcinogenesis. Cancer Res 2008;68:5049–58.
20. Pan Y, Claret FX. Targeting Jab1/CSN5 in nasopharyngeal carcinoma. Cancer Lett 2012;326:155–60.
21. Lujambio A, Calin GA, Villanueva A, Ropero S, Sanchez-Cespedes M, Blanco D, et al. A microRNA DNA methylation signature for human cancer metastasis. Proc Natl Acad Sci U S A 2008;105:13556–61.
22. Wang LQ, Liang R, Chim CS. Methylation of tumor suppressor microRNAs: lessons from lymphoid malignancies. Expert Rev Mol Diagn 2012;12:755–65.
23. Kozaki K, Imoto I, Mogi S, Omura K, Inazawa J. Exploration of tumor-suppressive microRNAs silenced by DNA hypermethylation in oral cancer. Cancer Res 2008;68:2094–105.
24. Vrba L, Jensen TJ, Garbe JC, Heimark RL, Cress AE, Dickinson S, et al. Role for DNA methylation in the regulation of miR-200c and miR-141 expression in normal and cancer cells. PLoS ONE 2010;5:e8697.
25. Chen H, Hutt-Fletcher L, Cao L, Hayward SD. A positive autoregulatory loop of LMP1 expression and STAT activation in epithelial cells latently infected with Epstein-Barr virus. J Virol 2003;77:4139–48.

26. Hino R, Uozaki H, Murakami N, Ushiku T, Shinozaki A, Ishikawa S, et al. Activation of DNA methyltransferase 1 by EBV latent membrane protein 2A leads to promoter hypermethylation of PTEN gene in gastric carcinoma. Cancer Res 2009;69:2766–74.
27. Qu CJ, Liang ZH, Huang JL, Zhao RY, Su CH, Wang SM, et al. MiR-205 determines the radioresistance of human nasopharyngeal carcinoma by directly targeting PTEN. Cell Cycle 2012;11:785–96.
28. Pogribny I, Yi P, James SJ. A sensitive new method for rapid detection of abnormal methylation patterns in global DNA and within CpG islands. Biochem Biophys Res Commun 1999;262:624–8.
29. Jacinto FV, Ballestar E, Esteller M. Methyl-DNA immunoprecipitation (MeDIP): hunting down the DNA methylome. Biotechniques 2008; 44:35, 37, 39.
30. Gehring M, Bubb KL, Henikoff S. Extensive demethylation of repetitive elements during seed development underlies gene imprinting. Science 2009;324:1447–51.
31. Huang J, Renault V, Sengenes J, Touleimat N, Michel S, Lathrop M, et al. MeQA: a pipeline for MeDIP-seq data quality assessment and analysis. Bioinformatics 2012;28:587–8.
32. Li LC, Dahiya R. MethPrimer: designing primers for methylation PCRs. Bioinformatics 2002;18:1427–31.
33. Lal A, Pan Y, Navarro F, Dykxhoorn DM, Moreau L, Meire E, et al. miR-24-mediated downregulation of H2AX suppresses DNA repair in terminally differentiated blood cells. Nat Struct Mol Biol 2009;16:492–8.
34. Kovalchuk O, Hendricks CA, Cassie S, Engelward AJ, Engelward BP. *In vivo* recombination after chronic damage exposure falls to below spontaneous levels in "recombomice." Mol Cancer Res 2004;2: 567–73.
35. Gibcus JH, Tan LP, Harms G, Schakel RN, de Jong D, Blokzijl T, et al. Hodgkin lymphoma cell lines are characterized by a specific miRNA expression profile. Neoplasia 2009;11:167–76.
36. Lin SC, Liu CJ, Lin JA, Chiang WF, Hung PS, Chang KW. miR-24 up-regulation in oral carcinoma: positive association from clinical and *in vitro* analysis. Oral Oncol 2010;46:204–8.
37. Wu J, Zhang YC, Suo WH, Liu XB, Shen WW, Tian H, et al. Induction of anion exchanger-1 translation and its opposite roles in the carcinogenesis of gastric cancer cells and differentiation of K562 cells. Oncogene 2010;29:1987–96.
38. Cheng AM, Byrom MW, Shelton J, Ford LP. Antisense inhibition of human miRNAs and indications for an involvement of miRNA in cell growth and apoptosis. Nucleic Acids Res 2005;33:1290–7.
39. Lal A, Navarro F, Maher CA, Maliszewski LE, Yan N, O'Day E, et al. miR-24 Inhibits cell proliferation by targeting E2F2, MYC, and other cell-cycle genes via binding to "seedless" 3′UTR microRNA recognition elements. Mol Cell 2009;35:610–25.
40. Mishra PJ, Song B, Mishra PJ, Wang Y, Humeniuk R, Banerjee D, et al. MiR-24 tumor suppressor activity is regulated independent of p53 and through a target site polymorphism. PLoS ONE 2009;4: e8445.
41. Helleday T, Lo J, van Gent DC, Engelward BP. DNA double-strand break repair: from mechanistic understanding to cancer treatment. DNA Repair 2007;6:923–35.
42. Meng F, Wehbe-Janek H, Henson R, Smith H, Patel T. Epigenetic regulation of microRNA-370 by interleukin-6 in malignant human cholangiocytes. Oncogene 2008;27:378–86.
43. Lujambio A, Esteller M. CpG island hypermethylation of tumor suppressor microRNAs in human cancer. Cell Cycle 2007;6: 1455–9.
44. Grady WM, Parkin RK, Mitchell PS, Lee JH, Kim YH, Tsuchiya KD, et al. Epigenetic silencing of the intronic microRNA hsa-miR-342 and its host gene EVL in colorectal cancer. Oncogene 2008;27:3880–8.
45. Pan C, Chen H, Wang L, Yang S, Fu H, Zheng Y, et al. Down-regulation of MiR-127 facilitates hepatocyte proliferation during rat liver regeneration. PLoS ONE 2012;7:e39151.
46. Chen Y, Luo J, Tian R, Sun H, Zou S. miR-373 negatively regulates methyl-CpG-binding domain protein 2 (MBD2) in hilar cholangiocarcinoma. Dig Dis Sci 2011;56:1693–701.
47. Cortez MA, Bueso-Ramos C, Ferdin J, Lopez-Berestein G, Sood AK, Calin GA. MicroRNAs in body fluids-the mix of hormones and biomarkers. Nat Rev Clin Oncol 2011;8:467–77.
48. Di Leva G, Croce CM. miRNA profiling of cancer. Curr Opin Genet Dev 2013;23:3–11.
49. Lu J, He ML, Wang L, Chen Y, Liu X, Dong Q, et al. MiR-26a inhibits cell growth and tumorigenesis of nasopharyngeal carcinoma through repression of EZH2. Cancer Res 2011;71:225–33.
50. Lanford RE, Hildebrandt-Eriksen ES, Petri A, Persson R, Lindow M, Munk ME, et al. Therapeutic silencing of MicroRNA-122 in primates with chronic hepatitis C virus infection. Science 2010; 327:198–201.
51. Janssen HLA, Reesink HW, Lawitz EJ, Zeuzem S, Rodriguez-Torres M, Patel K, et al. Treatment of HCV infection by targeting MicroRNA. N Engl J Med 2013;368:1685–94.